

Short communication

Electrochemical disproportionation in new ruthenium (II) nitro complexes with 2,4,6-tris(2-pyridyl)-1,3,5-triazine detected by IR spectroelectrochemistry with an OTTLE cell



Sofía E. Domínguez, Florencia Fagalde *

INQUINOA-CONICET, Instituto de Química Física, Facultad de Bioquímica, Química y Farmacia, Universidad Nacional de Tucumán, Ayacucho 471, T4000INI San Miguel de Tucumán, Argentina

ARTICLE INFO

Article history:

Received 23 November 2016

Accepted 14 January 2017

Available online 17 January 2017

Keywords:

Nitro polypyridyl ruthenium (II) complexes

tris(2-Pyridyl)-1,3,5-triazine

Nitrosyl complexes

FT-IR spectroelectrochemistry

ABSTRACT

The syntheses and characterization of new nitro complexes of Ru(II) with 2,4,6-tris(2-pyridyl)-1,3,5-triazine (tptz) and different substituted bipyridines are reported. A disproportionation reaction can occur after applying an oxidation potential corresponding to the couple Ru^{II}/Ru^{III} forming the nitrate and the nitrosyl complexes, which were detected by cyclic voltammetry. This reaction was confirmed by IR-spectroelectrochemistry with an OTTLE cell, for the first time. Additionally, for 2,2'-bipyridine we have obtained as ClO₄⁻ salt a new nitrosyl-complex which presents an elevated IR stretching frequency.

© 2017 Elsevier B.V. All rights reserved.

The reactivity of nitro complexes of palladium, rhodium, cobalt and ruthenium as oxygen atom transfer (OAT) agents is interesting because their potential applications like selective catalysts for oxidation of organic [1] and inorganic [2] substrates, which are relevant in chemical industry [3]. Also some iron-complexes with hemo and non-hemo ligands [4,5] are interesting because is potentially a physiological route of formation of nitric oxide. In addition, after the OAT reaction the nitrosyl-complex is obtained, and the initial nitro-complex could be regenerated.

Recently we have synthesized and characterized new nitro and nitrite complexes of ruthenium (I) [6], where we report through IR-spectroelectrochemistry, that an O-atom transfer reaction occurs triggered by oxidation of these complexes leading to a nitrosyl complex as a product [7]. In this work, we have extended our investigation to new nitro complexes of ruthenium of formulae: [Ru(tptz)(bpy)(NO₂)]PF₆ (**1**), [Ru(tptz)(dmb)(NO₂)]PF₆ (**2**), [Ru(tptz)(dcb)(NO₂)]PF₆ (**3**) (with tptz = 2,4,6-tris(2-pyridyl)-1,3,5-triazine; bpy = 2,2'-bipyridine; dmb = 4,4'-dimethyl-2,2'-bipyridine and dcb = 4,4'-dicarboxy-2,2'-bipyridine). Fig. 1 schematize their structures. Additionally, derived from complex (**1**), we have obtained the nitrosyl complex [Ru(tptz)(bpy)(NO)](ClO₄)₃ (**4**).

In concordance with nitro-complexes of Ru(III) [8–12], Os(III) [13] and Fe(III) [14] with polypyridil ligands, in this work we have detected for complex (**1**), the occurrence of a disproportionation reaction after an OAT giving the corresponding nitrosyl and nitrate complexes. This reaction was detected by cyclic voltammetry and, for the first time was confirmed by IR-spectroelectrochemistry with an OTTLE cell.

All chemicals used were analytical reagent grade, and were purchased from Sigma-Aldrich and used as received. 4,4'-dicarboxy-2,2'-bipyridine was prepared as previously reported [15]. UV-visible absorption spectra were recorded on a Varian Cary 50 spectrophotometer. IR spectra were obtained with a Perkin-Elmer Spectrum RX-1 FTIR spectrometer. Raman spectra were measured with a DXR Thermo Scientific spectrometer with an Olympus microscopy, using a 532 nm laser. Cyclic voltammetry (CV) and differential pulse voltammetry (DPV) experiments were carried out using BAS Epsilon EC equipment, with vitreous C as working electrode, Pt wire as auxiliary electrode, and Ag/AgCl (3 M NaCl) as reference electrode. For DPV the pulse amplitude was 50 mV, the pulse width was 50 ms and the pulse period was 200 ms. Acetonitrile was freshly distilled over P₄O₁₀ for electrochemical measurements. Tetrakis(*n*-butyl)ammoniumhexafluorophosphate (TBAH) was dried at 150 °C for 24 h before being used as supporting electrolyte. The solutions used in voltammetry in the cathodic region were degassed with Ar prior each measurement. An IR OTTLE cell [16] was employed equipped with CaF₂ windows and a Pt-minigrad working electrode, a Pt-minigrad as auxiliary electrode and Ag wire pseudo-reference electrode. Controlled potential electrolyses within the OTTLE cell were carried out using a Teq-04 potentiostat. For spectroelectrochemistry experiments the concentrations of the complexes were 3.10⁻³ M and 0.3 M TBAH. The measurements were done applying 100 mV steps potential, and when the initial spectrum began to change the steps were of 50 mV. After that, the potential at each step was maintained until the spectrum does not change anymore and then a new step was applied. The application of potential in small steps was done in order to avoid high electrolytic currents *i*_c and uncontrolled potential shifts due to a large ohmic potential drop *i*_cR (ΔE = E_{app1} - *i*_cR) [17]. The range

* Corresponding author.

E-mail address: ffagalde@fbqf.unt.edu.ar (F. Fagalde).

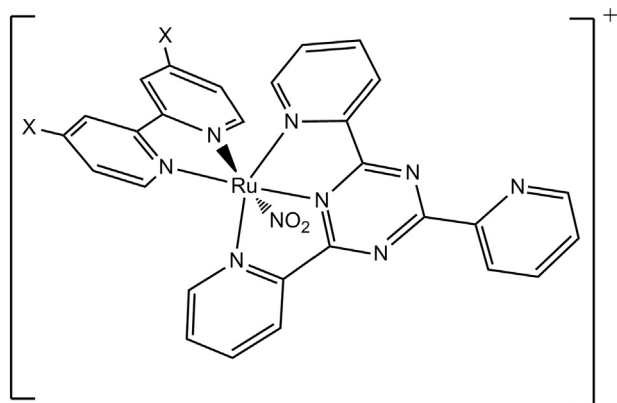


Fig. 1. Nitro-complexes under investigation where X = H (bpy), $-\text{CH}_3$ (dmb) and $-\text{COOH}$ (dcb), in all cases counterion = PF_6^- .

of potential employed were $0 < E < 2$ V for the oxidation region. Chemical analyses for C, H and N were carried out at INQUIMAE, University of Buenos Aires, Argentina, with an estimated error of $\pm 0.5\%$.

DFT and TD-DFT calculations were done using Gaussian 03 [18]. Molecules were optimized using the hybrid functional B3LYP [19]. Basis set LanL2DZ [20] was chosen for all atoms, and geometry optimizations were performed in the gas phase. Frequency calculations were performed to ensure that these geometries corresponded to global minima: no imaginary frequencies were obtained for the optimized geometries. The effect of the solvent was included using the polarizable continuum model (CPCM) [21] for calculating orbital energy levels and UV–vis spectra in CH_3CN . The contribution of the different groups on the orbitals, calculated UV–vis spectra, and transition related to them were obtained using the GaussSum 3.0 Software [22].

The syntheses of chloro- and aqua-complexes were done according to literature [23] and will be reported in a separate manuscript [24]. Nitro-complexes were synthesized with slight modifications in protocols already reported [25].

Complex (1). $[\text{Ru}(\text{tptz})(\text{bpy})(\text{H}_2\text{O})](\text{PF}_6)_2$ (50 mg, 0.057 mmol) and NaNO_2 (47 mg; 0.684 mmol) were dissolved in 12 mL of acetone and 8 mL of water. The purple solution was heated at reflux for 3 h under Ar with stirring and protected from light exposure thought an aluminum foil. During that time the solution turned red-orange. After cooling at room temperature, the acetone was rotoevaporated and a dark orange solid precipitated. The suspension was transfer to a beaker and NH_4PF_6 (60 mg dissolved in 1 mL of water) was added and the mixture was cooling in the refrigerator for c.a. 2–3 h. The resulting solid was collected by filtration and washed with minimum amount of cold water and dry under vacuum over P_4O_{10} . Yield: 40 mg (92%). Chemical analyses were coherent with the formula $[\text{Ru}(\text{tptz})(\text{bpy})(\text{NO}_2)]\text{PF}_6 \cdot \text{H}_2\text{O}$. Chem. Anal. Calc. for $\text{C}_{28}\text{H}_{22}\text{N}_9\text{O}_3\text{PF}_6\text{Ru}$: C, 43.2; H, 2.8; N, 16.2%. Found: C, 43.2; H, 2.7; N, 16.2%.

Complex (2). The synthesis was done with the same procedure as before from 50 mg of $[\text{Ru}(\text{tptz})(\text{dmb})(\text{H}_2\text{O})](\text{PF}_6)_2 \cdot 2\text{H}_2\text{O}$ (0.053 mmol) and 44 mg of NaNO_2 (0.637 mmol). Yield: 40 mg (92%). Chemical analyses were coherent with the formula $[\text{Ru}(\text{tptz})(\text{dmb})(\text{NO}_2)]\text{PF}_6 \cdot 2.5\text{H}_2\text{O}$. Chem. Anal. Calc. for $\text{C}_{30}\text{H}_{29}\text{N}_9\text{O}_{4.5}\text{PF}_6\text{Ru}$: C, 43.2; H, 3.5; N, 15.1%. Found: C, 43.1; H, 3.6; N, 14.4%.

Complex (3). The synthesis was done with the same procedure from 40 mg of $[\text{Ru}(\text{tptz})(\text{dcb})(\text{H}_2\text{O})](\text{PF}_6)_2 \cdot 0.5\text{H}_2\text{O}$ (0.041 mmol) and 42 mg of NaNO_2 (0.612 mmol) dissolved in 15 mL of acetone and 8 mL of water. Yield: 14 mg (33%). Chemical analyses were coherent with the formula $[\text{Ru}(\text{tptz})(\text{dcb})(\text{NO}_2)]\text{PF}_6 \cdot 10\text{H}_2\text{O}$. Chem. Anal. Calc. for $\text{C}_{30}\text{H}_{40}\text{N}_9\text{O}_{16}\text{PF}_6\text{Ru}$: C, 35.0; H, 3.9; N, 12.2%. Found: C, 35.0; H, 3.0; N, 12.2%.

Complex (4). $[\text{Ru}(\text{tptz})(\text{bpy})(\text{NO}_2)]\text{PF}_6 \cdot \text{H}_2\text{O}$ (25 mg, 0.033 mmol) was dissolved with 3 mL of acetone. The resulting dark orange-red

solution was cooled in an ice bath and 1 mL of 6 M HClO_4 was added, maintaining the solution in the bath under stirring for 1 h. After that time the solution turned dark purple-pink. 2 mL of an aqueous solution of NaClO_4 was added. The acetone was evaporated in air under hood protected of light. It was observed the formation of a precipitate however the solution keeps colored. The small quantity of solid was filtered off, washed with a minimum amount of cold 0.1 M HClO_4 and dry under vacuum over P_4O_{10} . Yield: 2 mg (7%). In a second attempt to obtain greater amount of precipitate, the solid decomposed possibly due to protonation of the nitrogens atoms of pyridine and triazine in the tptz ligand, resulting in a very low yield. *Caution: sodium perchlorate, perchloric acid and perchlorate salts of metal complexes with organic ligands are potentially explosive. All these compounds should be handled in small quantities, using the appropriate safety procedures* [26].

IR and Raman spectra of complexes (1) to (3) display the characteristic vibration modes for polypyridyl and triazine ligands between 1600 and 400 cm^{-1} , and the stretching frequencies of the nitro ligand $\nu_a(\text{NO}_2^-)$ and $\nu_s(\text{NO}_2^-)$ [27] (Supplementary Fig. S1 and Supplementary Table S1). These results indicate that the nitrite ion is coordinated through the N-atom resulting in the so-called nitro or N-nitrite isomer for the three compounds in contrast with rhenium(I) tricarbonyl complexes with bpy and dmb where the nitrite ion is coordinated through its N- and O- atom respectively [6].

Complex (4) shows an intense band at 1943 cm^{-1} corresponding to the stretching frequencies ν_{NO} (Supplementary Fig. S2). The value of ν_{NO} found for complex (4) indicates a strong character of nitrosonium cation, being NO^+ a limiting case affording a triple N—O bond order [29]. According to the Enemark-Feltham formalism complex (4) could be described as $\{\text{RuNO}\}^6$ [28].

The UV–visible spectra for complexes (1) to (3) in CH_3CN are shown in Supplementary Fig. S3. Two metal-to-ligand charge transfer transition (MLCT) from $d\pi$ orbital of Ru to π^* orbitals of the polypyridine ligands in concordance with similar complexes [25,30–31]. The lower energy band is assigned to $d\pi \rightarrow \pi^*(\text{tptz})$, and the next band correspond to $d\pi \rightarrow \pi^*(\text{X}_2\text{-bpy})$. This assignation was confirmed by TD-DFT calculations (vide infra). The high energy bands between 250 and 300 nm are ligand centered (LC) due to $d\pi \rightarrow \pi^*$ transitions.

Table 1 shows the electrochemical data for complexes (1) to (3) in CH_3CN , using 0.1 M TBAH as supporting electrolyte. Supplementary Fig. S4 shows for complex (2) the CV and DPV in the cathodic region. As in complex (1) and (3), three reduction waves appear. The first one corresponds to a reversible process and the second is quasi-reversible. However, when the potential sweep is done between 0 and -2 V, the inverse waves are not observed because the third reduction process is irreversible. In all cases, the first and third reductions are assigned to the tptz ligand and are shifted to lower values with respect to the free tptz ($E_1 \approx -1.4 / -1.5$ V and $E_2 \approx -2.1$ V vs Ag/AgCl) [31–35], because the coordination with the metal center stabilizes the π^* orbitals of the tptz ligand. On the other hand the second reduction wave is assigned to the bipyridine ligand. It was found that as greater is the π -backbonding ($\text{dcb} > \text{bpy} > \text{dmb}$) the reduction potential corresponding to this ligand is lower, because of the stabilization of the π^* orbitals, in agreement with previous reports for complexes with substituted bipyridines with different π -acceptor capabilities [36].

In the anodic region, it was observed a wave corresponding to the $\text{Ru}^{\text{II}}/\text{Ru}^{\text{III}}$ couple (Table 1). For complex (1), as seen in Fig. 2a the electrochemical process is irreversible and indicates the decomposition of the complex. Moreover, in the DPV shown in Fig. 2b a second peak is clearly observed at higher potentials, which can be assigned to the oxidation of complex (1). Additionally, on the reductive sweep of the cyclic voltammograms two waves of low intensity of current appear at $E_{1/2} = 0.58$ V and $E_{\text{peak}} = 0.2$ V. According to literature [31], these reductions are assigned to the nitrosyl ligand, and corresponds to the $\{\text{RuNO}\}^6/\{\text{RuNO}\}^7/\{\text{RuNO}\}^8$ couples which could be expressed in a simplified limiting manner as $\text{NO}^+/\text{NO}^\bullet/\text{NO}^-$. These potential values are also correlated with the high frequency ν_{NO} found for the complex. This assignment

Table 1Electrochemical data for complexes (1) to (3), obtained from CV in 0.1 M TBAH in CH₃CN at 100 mV/s. Potential values are referred to Ag/AgCl (3 M NaCl). $E_{1/2} = (E_c + E_a)/2$.

Complex	$E_{\text{peak}} \text{Ru}^{\text{II}}/\text{Ru}^{\text{III}}$	$E_{1/2} \text{tptz}/\text{tptz}^{\bullet-} (\Delta E)$	$E_{\text{peak}} \text{LL}/\text{LL}^{\bullet-}$	$E_{\text{peak}} \text{tptz}^{2-}/\text{tptz}^{\bullet-}$
(1)	1.29 V	−0.80 V (85 mV)	−1.34 V	−1.85 V
(2)	1.26 V	−0.81 V (84 mV)	−1.58 V	−1.90 V
(3)	1.40 V	−0.79 V (60 mV)	−1.06 V	−1.80 V

was confirmed by IR-spectroelectrochemistry and will be discussed in the next section. Additionally, as seen in Fig. 2a, the oxidation wave at $E_{\text{peak}} = 1.29$ V, corresponding to the Ru^{II}/Ru^{III} couple, disappear in the second cycle of the voltammetry, indicating that there is a chemical reaction coupled to the electrochemical reaction by which complex (1) decomposes. As was mentioned before, for other nitro-complexes of ruthenium [8–12], osmium [13] and iron [14] the coordinated nitrite ion disproportionate upon oxidation producing the corresponding nitrosyl and nitrate complexes. Besides, the second oxidation wave observed in the voltammogram ($E_p = 1.38$ V) could be assigned to the Ru^{II}/Ru^{III} couple of the nitrate-complex [Ru^{II}(tptz)(bpy)(NO₃)⁺]⁺ obtained, because the potential values are close to the nitro-complex (1.29 V). This wave cannot be assigned to the Ru^{II}/Ru^{III} couple of the nitrosyl complex because a higher value is expected due to the better π -acceptor ability of the nitrosyl ligand with respect to nitrite and nitrate.

For complex (2) (Supplementary Fig. S5) it appears a low intense wave at $E_{1/2} \approx 0.6$ V which can be also assigned to the nitrosyl-complex. However, the Ru^{II}/Ru^{III} couple of the nitro-complex electrogenerated is more reversible than for complex (1) showing that the disproportionate reaction occurs to a lesser extent possible due to the donor effect of the methyl substituent in accordance with Meyer et al. [9,13,].

In Supplementary Fig. S6 is shown the mechanism proposed for the disproportionation reaction for nitro-complexes of Ru (II) after oxidation to Ru (III) in concordance with previous reports by Meyer [9,13, 37], where the rate determinant step is the bimolecular process. Thus, the low intensity of the reduction wave of nitrosyl could be due to a steric effect originated in the voluminous ligand tptz that would not favor the formation of the dimeric species so the disproportionate reaction occurs in low magnitude.

Fig. 3a shows the IR spectra obtained when a potential of $E = 1.2$ V was applied to a solution of complex (1). It is observed a small band at around 1950 cm^{−1} corresponding to the ν_{NO} stretching frequency of complex (4). The low intensity found for this band is related with a small quantity of product obtained and agrees with the low intensity of the reduction wave observed in the CV (Fig. 2a). Moreover, when a potential $E = 0$ V was applied (Fig. 3b) the band at 1950 cm^{−1}

disappears in agreement with the reduction localized in the nitrosyl ligand, verifying these assignment. The new band corresponding to the species {RuNO}⁷ (NO• in a simplified notation) that should appear at around 1600–1700 cm^{−1}, was not visualized due to the absorption of the solvent in that spectral region (Spectra from 4000 to 1000 cm^{−1} in Supplementary information Fig. S7).

For complex (2), the band corresponding to nitrosyl stretching frequency ν_{NO} was not observed because the quantity of the nitrosyl complex would be too small to be detected in the measurement conditions, in concordance with the disproportionate reaction which occurs in a lower magnitude than in complex (1).

Computational analyses were carried out for complexes (1) and (2) and are shown in Supplementary Information. DFT calculated energies and compositions of selected molecular orbitals expressed in terms of composing fragments for complexes (1) and (2) are shown in Supplementary Table S2. Supplementary Fig. S8 shows the frontier orbitals for both complexes. The HOMO, HOMO-1 and HOMO-2 are predominantly based in $d\pi$ orbitals of the Ru atom. The LUMO and LUMO+1 are π^* orbitals primarily localized on the tptz ligand, while LUMO+2 is a π^* orbital based on the bipyridine ligand. This last orbital is at high energy for complex (2) than for complex (1), due to the lower π -accepting ability of dmb versus bpy.

Supplementary Table S3 summarized the TD-DFT calculated energies of low-lying singlet electronic transitions for complexes, the oscillator strengths and the experimental values which able us to confirm the assignments of the electronic transitions.

To conclude, we have synthesized three new Ru(II) nitro-complexes with the tridentate ligand tptz and the bidentate ligands bpy, dmb and dcb which have different abilities to accept electronic density from the metal center. The spectroscopic and electrochemical properties of the complexes were characterized. Besides, we have obtained the nitrosyl complex with a high stretching frequency, ν_{NO} . For complex (1) it was found an electrochemical disproportionation reaction to give the nitrate and nitrosyl-complexes, which was confirmed by IR spectroelectrochemistry. For complex (2), this reaction also occurs but in lower magnitude. DFT and TD-DFT confirm the assignment of the absorption bands observed in the UV–visible spectra.

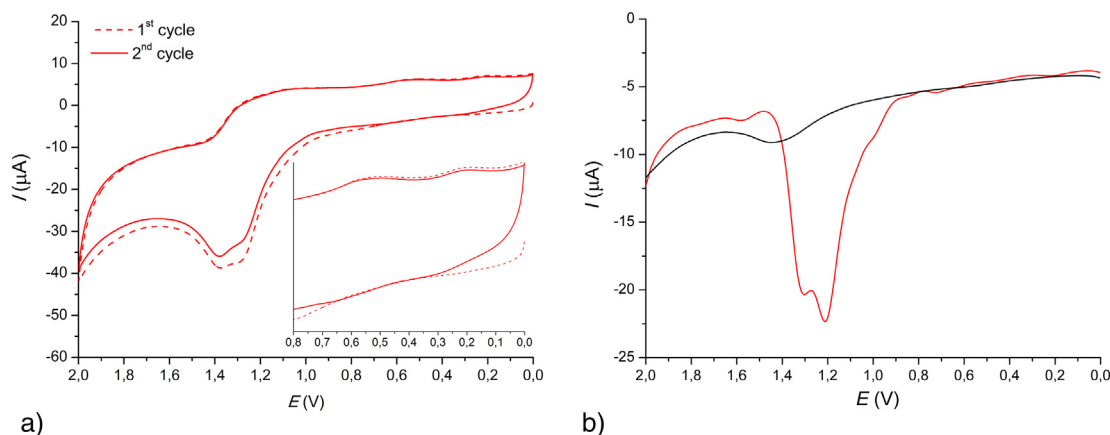


Fig. 2. (a) Cyclic voltammetry at 100 mV·s^{−1} (left) and (b) differential pulse voltammetry (right) in the anodic region, for complex (1) $C = 1.10^{-3}$ M in CH₃CN using 0.1 M TBAH as supporting electrolyte.

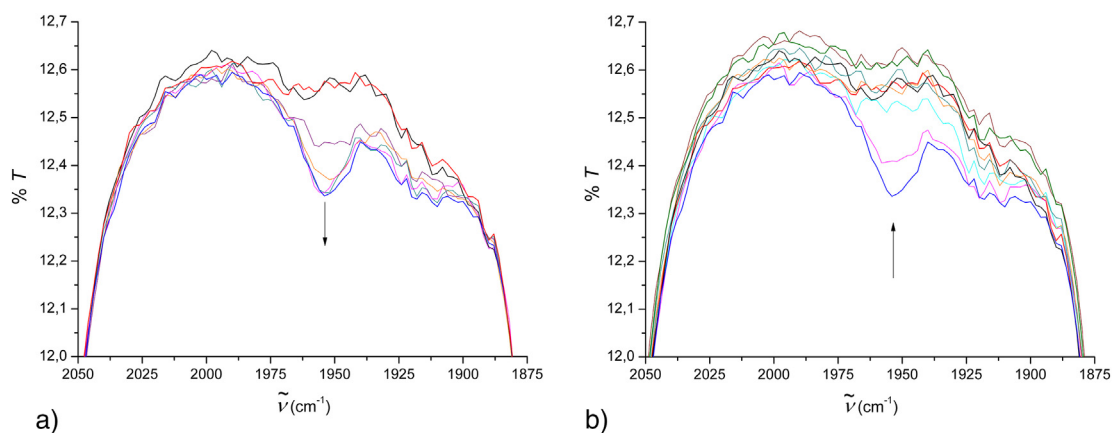


Fig. 3. FT-IR spectroelectrochemistry for complex (**1**), $C = 3.10^{-3}$ M in CH_3CN with 0.3 M TBAH. Spectra from 2050 to 1875 cm^{-1} . (a) $E = 1.2$ V, $\Delta t \approx 2$ min. (b) $E = 0$ V, $\Delta t \approx 2$ min. The black line is the supporting electrolyte. Red line is the initial spectra of complex (**1**), without applying an external potential. Blue line is the final spectra of electrolyses after applying a potential $E = 1.2$ V, $\Delta t \approx 2$ min (left). Green line is the final spectra of electrolyses after applying a potential $E = 0$ V, $\Delta t \approx 2$ min (right). (For interpretation of the references to colour in this figure legend, the reader is referred to the web version of this article.)

Acknowledgment

We thank Universidad Nacional de Tucumán (UNT, PIUNT D547/1), Consejo Nacional de Investigaciones Científicas y Técnicas (CONICET, PIP 11220110100916), and Agencia Nacional de Promoción Científica y Tecnológica (ANPCyT, PICT 1553-2011), all from Argentina, for financial support. F.F. is Member of the Research Career from CONICET, Argentina.

Appendix A. Supplementary material

IR, Raman, UV–vis, CV and DPV, spectroelectrochemical measurements, scheme of disproportionation and computational data are available as Supporting Information. Supplementary data associated with this article can be found in the online version, at <http://dx.doi.org/10.1016/j.inoche.2017.01.020>.

References

- [1] R.A. Leising, K.J. Takeuchi, *J. Am. Chem. Soc.* 110 (1988) 4079 (and references herein).
- [2] (a) B.S. Tovrog, S.E. Diamond, F. Mares, *J. Am. Chem. Soc.* 101 (1979) 270; (b) K. Yamamoto, *Polyhedron* 5 (1986) 913.
- [3] J.P. Solar, F. Mares, S.E. Diamond, *Catal. Rev.* 27 (1985) 1.
- [4] P.C. Ford, *Inorg. Chem.* 49 (2010) 6226.
- [5] J. Heinecke, P.C. Ford, *Coord. Chem. Rev.* 254 (2010) 235.
- [6] S.E. Domínguez, F. Fagalde, *Polyhedron* 67 (2014) 471.
- [7] S.E. Domínguez, F. Fagalde, *Polyhedron* 100 (2015) 114.
- [8] F.R. Keene, D.J. Salmon, J.L. Walsh, H.D. Abruña, T.J. Meyer, *J. Am. Chem. Soc.* 99 (1977) 2384.
- [9] F.R. Keene, D.J. Salmon, J.L. Walsh, H.D. Abruña, T.J. Meyer, *Inorg. Chem.* 19 (1980) 1896.
- [10] H. Nagao, M. Mukaida, K. Shimizu, F.S. Howell, H. Kakihana, *Inorg. Chem.* 25 (1986) 4312.
- [11] R.A. Leising, S.A. Kubow, L.F. Szczepura, K.J. Takeuchi, *Inorg. Chim. Acta* 245 (1996) 167.
- [12] L.F. Szczepura, S.A. Kubow, R.A. Leising, W.J. Perez, M.H.V. Huynh, C.H. Lake, D.G. Churchill, M.R. Churchill, K.J. Takeuchi, *J. Chem. Soc. Dalton Trans.* (1996) 1463.
- [13] D.W. Pipes, T.J. Meyer, *Inorg. Chem.* 23 (1984) 2466.
- [14] M.G. Finnegan, A.G. Lappin, W.R. Scheidt, *Inorg. Chem.* 29 (1990) 181.
- [15] F.H. Case, *J. Am. Chem. Soc.* 68 (1946) 2574.
- [16] M. Krejčík, M. Daněk, F. Hartl, J. Electroanal. Chem. 317 (1991) 179.
- [17] F.P.A. Johnson, M.W. George, F. Hartl, J.J. Turner, *Organometallics* 15 (1996) 3374.
- [18] M.J. Frisch, G.W. Trucks, H.B. Schlegel, G.E. Scuseria, M.A. Robb, J.R. Cheeseman, J.A. Montgomery Jr., T. Vreven, K.N. Kudin, J.C. Burant, J.M. Millam, S.S. Iyengar, J. Tomasi, V. Barone, B. Mennucci, M. Cossi, G. Scalmani, N. Rega, G.A. Petersson, H. Nakatsuji, M. Hada, M. Ehara, K. Toyota, R. Fukuda, J. Hasegawa, M. Ishida, T. Nakajima, Y. Honda, O. Kitao, H. Nakai, M. Klene, X. Li, J.E. Knox, H.P. Hratchian, J.B. Cross, C. Adamo, J. Jaramillo, R. Gomperts, R.E. Stratmann, O. Yazyev, A.J. Austin, R. Cammi, C. Pomelli, J.W. Ochterski, P.Y. Ayala, K. Morokuma, G.A. Voth, P. Salvador, J.J. Dannenberg, V.G. Zakrzewski, S. Dapprich, A.D. Daniels, M.C. Strain, O. Farkas, D.K. Malick, A.D. Rabuck, K. Raghavachari, J.B. Foresman, J.V. Ortiz, Q. Cui, A.G. Baboul, S. Clifford, J. Cioslowski, B.B. Stefanov, G. Liu, A. Liashenko, P. Piskorz, I. Komaromi, R.L. Martin, D.J. Fox, T. Keith, M.A. Al-Laham, C.Y. Peng, A. Nanayakkara, M. Challacombe, P.M.W. Gill, B. Johnson, W. Chen, M.W. Wong, C. Gonzalez, J.A. Pople, Gaussian 03, Revision C.02, Gaussian Inc., Wallingford CT, 2004.
- [19] (a) A.D. Becke, *J. Chem. Phys.* 98 (1993) 5648; (b) C. Lee, W. Yang, R.G. Parr, *Phys. Rev. B* 37 (1988) 785.
- [20] (a) P.J. Hay, W.R. Wadt, *J. Chem. Phys.* 82 (1985) 270; (b) W.R. Wadt, P.J. Hay, *J. Chem. Phys.* 82 (1985) 284; (c) P.J. Hay, W.R. Wadt, *J. Chem. Phys.* 82 (1985) 299.
- [21] M. Cossi, N. Rega, G. Scalmani, V. Barone, *J. Comput. Chem.* 24 (2003) 669.
- [22] N.M. O'Boyle, A.L. Tenderholt, K.M. Langner, *J. Comput. Chem.* 29 (2008) 839.
- [23] (a) B.P. Sullivan, J.M. Calvert, T.J. Meyer, *Inorg. Chem.* 19 (1980) 1404; (b) D.C. Ware, P.A. Lay, H. Taube, *Inorg. Synth.* 24 (1986) 299.
- [24] S.E. Domínguez, PhD Thesis Lic. Universidad Nacional de Tucumán, 2016.
- [25] M. Videla, J.S. Jacinto, R. Baggio, M.T. Garland, P. Singh, W. Kaim, L.D. Slep, J.A. Olabe, *Inorg. Chem.* 45 (2006) 8608.
- [26] W.C. Wolsey, *J. Chem. Educ.* 50 (1973) A335.
- [27] K. Nakamoto, *Infrared and Raman Spectra of Inorganic and Coordination Compounds*, fourth ed. Wiley, New York, 1986.
- [28] (a) J.H. Enemark, R.D. Feltham, *Coord. Chem. Rev.* 13 (1974) 339 ((b) nitrosyl species are described as $\{\text{MNO}\}^n$ (regardless of the coligands), where n stands for the number of d electrons in the metal (M) and the electrons in the $\pi^*(\text{NO})$ orbitals).
- [29] F. Roncaroli, M. Videla, L.D. Slep, J.A. Olabe, *Coord. Chem. Rev.* 251 (2007) 1903.
- [30] P. Paul, B. Tyagi, A.K. Bilakhiya, P. Dastidar, E. Suresh, *Inorg. Chem.* 39 (2000) 14.
- [31] S. Ghuman, S. Kar, S.M. Mobin, B. Harish, V.G. Puranik, G.K. Lahiri, *Inorg. Chem.* 45 (2006) 2413.
- [32] R.M. Berger, J.R. Holcombe, *Inorg. Chim. Acta* 232 (1995) 217.
- [33] N.E. Tokel-Takvoryan, R.E. Hemingway, A.J. Bard, *J. Am. Chem. Soc.* 95 (1973) 6582.
- [34] P. Paul, B. Tyagi, M.M. Bhadbhade, E. Suresh, *J. Chem. Soc. Dalton Trans.* (1997) 2273.
- [35] T. Saji, S. Aoyagui, *J. Electroanal. Chem.* 110 (1980) 329.
- [36] L.A. Worl, R. Duesing, P. Chen, L. Della Ciana, T.J. Meyer, *J. Chem. Soc. Dalton Trans.* (1991) 849.
- [37] R.W. Callahan, T.J. Meyer, *Inorg. Chem.* 16 (1977) 574.